# ACCELERATION INDUCED NEUTRON EMISSION IN HEAVY NUCLEI

**N. Carjan**[1,2], **M. Rizea**[2]

[1]Joint Institute for Nuclear Research, FLNR, 141980 Dubna, Moscow Region, Russia
[2]"Horia Hulubei" National Institute for Physics and Nuclear Engineering, Str. Reactorului no.30, P.O.BOX MG-6, Bucharest - Magurele, Romania

## Abstract

The effect of the acceleration of a nucleus on the neutron states is studied in the frame of the independent-particle nuclear shell model. For this we solve numerically the time-dependent Schrödinger equation, with a moving mean-field of Woods-Saxon type. The time evolution of a neutron states at the Fermi level is calculated for $^{236}U$ and acceleration parameter A=0.5 (in $10^{44}$ [fm/sec$^2$]). It is roughly the acceleration during the Coulomb repulsion of two $^{236}U$ nuclei when they are 20 fm apart. We keep this acceleration constant for $10^{-21}$ sec before we switch it off (A=0) and follow the wave packet for another $10^{-21}$ sec. During the acceleration, the wave function oscillates with increasing amplitude until it escapes, mainly in the direction opposite to the motion of the nucleus. The mean value of its energy (in the nuclear system) increases from -4.80 MeV to -3.15 MeV and 12% of the wave packet leave the nucleus. During the uniform motion, the wave packet continues to oscillate and to escape at a lower rate: an extra 2%. We repeated the calculations for two neighbouring states and found the emission rate to depend strongly on the position of the neutron state with respect to the Fermi energy. Finally, the effect of the nuclear deformation on the acceleration induced neutron emission is studied. In this case the period of oscillation is larger and the amplitude smaller. The angular distribution with respect to the direction of motion is also different: it has, in the nuclear system, an intense component almost perpendicular to the deformation axis.

## 1. Introduction

What if, like a fully-filled water tank, a nucleus will spill its less bound nucleons when accelerated? Most probable this could happen to neutrons since, contrary to protons, they are not protected by a Coulomb barrier. In case the answer is "yes", we are dealing with a new nuclear process. To give a first answer to this captivating question we choose a simple framework: the independent particle shell model [1]. We therefore solve the time-dependent Schrödinger equation with a moving mean-field of Woods-Saxon type and study the change in the neutron eigenstates during $10^{-21}$ sec of constant acceleration followed by $10^{-21}$ sec of constant velocity. This scenario is borrowed from the design of a linear accelerator [2].

The motion of a quantum particle in a moving one-dimensional potential well has been already studied in the field of control systems. Controlability is a mathematical concept that, in very generals terms, means the ability to do whatever we want with a given dynamical system; in particular, to transfer a quantum system from any initial state to any final state [3, 4] or to manipulate the position of a nano-particle using dynamical potential traps [5].

## 2. Formalism

In our case, we consider a neutron in a moving nuclear potential that has axial symmetry. It is represented by a wave function solution of the Schrödinger equation

$$i\hbar\frac{\partial\Theta(\rho,z,t)}{\partial t} = \mathcal{H}(\rho,z,t)\Theta(\rho,z,t), \tag{1}$$

where $\mathcal{H}$ is the single-particle Hamiltonian.

$$\mathcal{H} = -\frac{\hbar^2}{2m}\left[\frac{1}{\rho}\frac{\partial}{\partial\rho} + \frac{\partial^2}{\partial\rho^2} + \frac{\partial^2}{\partial z^2} - \frac{\Lambda^2}{\rho^2}\right] + V(\rho, z-\alpha(t)).$$

$\alpha(t)$ describes the displacement of the potential in time along the $z$ axis. $\Lambda$ is the projection of the orbital angular momentum on the symmetry axis. For simplicity the spin-orbit term is neglected.

By the Liouville transformation $\Phi = \rho^{1/2}\Theta$, the first derivative with respect to $\rho$ from $\mathcal{H}$ is removed, resulting a simplified Hamiltonian $H$ of the form:

$$H = -\frac{\hbar^2}{2m}\left[\frac{\partial^2}{\partial\rho^2} + \frac{\partial^2}{\partial z^2} - \frac{\Lambda^2 - 1/4}{\rho^2}\right] + V(\rho, z-\alpha(t)).$$

One arrives to the equation

$$i\hbar\frac{\partial\Phi(\rho,z,t)}{\partial t} = H(\rho,z,t)\Phi(\rho,z,t). \tag{2}$$

To solve this equation, a transformation of both the variable and the function from the non-inertial (laboratory) to the inertial (nuclear) system is convenient. It avoids an interpolation of the potential between the grid points at each time step.

We will explain this transformation on the 1-D TDSE:

$$i\hbar\frac{\partial\Phi(t,z)}{\partial t} = -\frac{h^2}{2m}\frac{\partial^2\Phi(t,z)}{\partial z^2} + V(z-\alpha(t))\Phi(t,z) \tag{3}$$

We go in the nuclear frame by the following changes of the variable $z \to q$ and of the function $\Phi \to \Psi$ [6]:

$$q = z - \alpha(t), \quad \Phi(t,z) = \exp(u)\Psi(t,q) \tag{4}$$

where

$$u = ib\left(z\dot{\alpha} - \alpha\dot{\alpha} + \frac{1}{2}\int_0^t \dot{\alpha}^2(t')dt'\right).$$

By taking $b = \frac{m}{\hbar}$, it can be shown that Eq.(3) will be transformed in

$$i\hbar\frac{\partial\Psi(t,q)}{\partial t} = -\frac{h^2}{2m}\frac{\partial^2\Psi(t,q)}{\partial q^2} + V(q)\Psi(t,q) + mq\ddot{\alpha}(t)\Psi(t,q). \tag{5}$$

To eliminate the linear term in $q$ (which tends to $\infty$ as $q \to \infty$), a further function transformation is performed [7]

$$\Psi(t,q) = \exp\left(-i\frac{\lambda}{\hbar}\right)\chi(t,q) \tag{6}$$

with

$$\lambda(t,q) = qm\int_0^t \ddot{\alpha}(t')dt' = q\beta(t).$$

In our particular case $\alpha(t) = \frac{1}{2}At^2$.

$$\dot{\alpha} = At, \ddot{\alpha} = A, \lambda = Bqt, B = mA$$

$$u = ib\left(zAt - \frac{1}{3}A^2t^3\right)$$

and the equation for $\chi$ is:

$$i\hbar\frac{\partial\chi(t,q)}{\partial t} = -\frac{h^2}{2m}\left(\frac{\partial^2\chi(t,q)}{\partial q^2} + \frac{2}{\hbar i}Bt\frac{\partial\chi(t,q)}{\partial q} - \frac{1}{\hbar^2}B^2t^2\chi(t,q)\right) + V(q)\chi(t,q). \qquad (7)$$

The advantage of these transformations is that they lead to equations in which the potential depends on a time-independent variable, the dependence on $\alpha(t)$ being transferred in the coefficients of Eqs.(5),(7).

## 3. Computational aspects

We work with the variables $\rho$ and $q$ on a finite numerical grid: [0,160]x[-256,256], $\Delta\rho = \Delta q$ =1/8 fm, $\Delta t$ =1/128 $\times 10^{-22}$ sec. The equations (5) and (7) are solved numerically by the Crank-Nicolson method. One obtains a linear system which is solved by a routine based on the Strong Implicit Procedure [8]. As initial solutions (at $t = 0$) we consider eigenfunctions of the original Hamiltonian.

The propagation in time is done in two steps. We consider a quadratic $\alpha$(t) and use Eq.(7) for $10^{-21}$ sec. Then we consider a linear $\alpha$(t) and use Eq.(5) without the $\ddot{\alpha}$ term for another $10^{-21}$ sec. At any time, by performing the inverse tranformations, we can retrieve the solution $\Phi(\rho, z, t)$ of the original equation. For the 1st step we choose the constant acceleration A=0.5[$10^{44} fm/sec^2$] resulting a constant velocity $v$=5[$10^{22} fm/sec$] for the 2nd step.

## 4. Results

As an example we take spherical $^{236}U$ and study 3 neutron states with $\Lambda$=0 around the Fermi level. The parameters of the Woods-Saxon potential are fitted to single-particle and single-hole states in the $^{208}$Pb region [9].

Fig.1 shows the result for the 14th eigenstate laying at -4.8 MeV. For T $>$ 0, the wave packet exhibits a changing asymmetry with respect to the $\rho$ axis indicative of an oscillation. In fact, we are dealing with an oscillation over the usual vibration of a quasi-stationary state. A similar vibration causes the barrier asaults in the Gamow picture of $\alpha$ decay [10]. The presence of the neutron inside the nucleus, measured by $N_{in}$, decreases from 1.00 (at T=0) to 0.88 (at T=10). A neutron, initially occupying this state, has therefore 12% chance to be emitted during the acceleration phase. For T $>$ 10 the oscillatory motion continues. At T=20 $N_{in}$ reaches an even lower value (0.86) because at T=10 the wave packet has short unbound tails which inevitably leave the nucleus.

The most probable direction of emission is 180° with respect to the displacement of the nucleus as in classical mechanics. There is however a weaker branch at $\approx$ 150° which

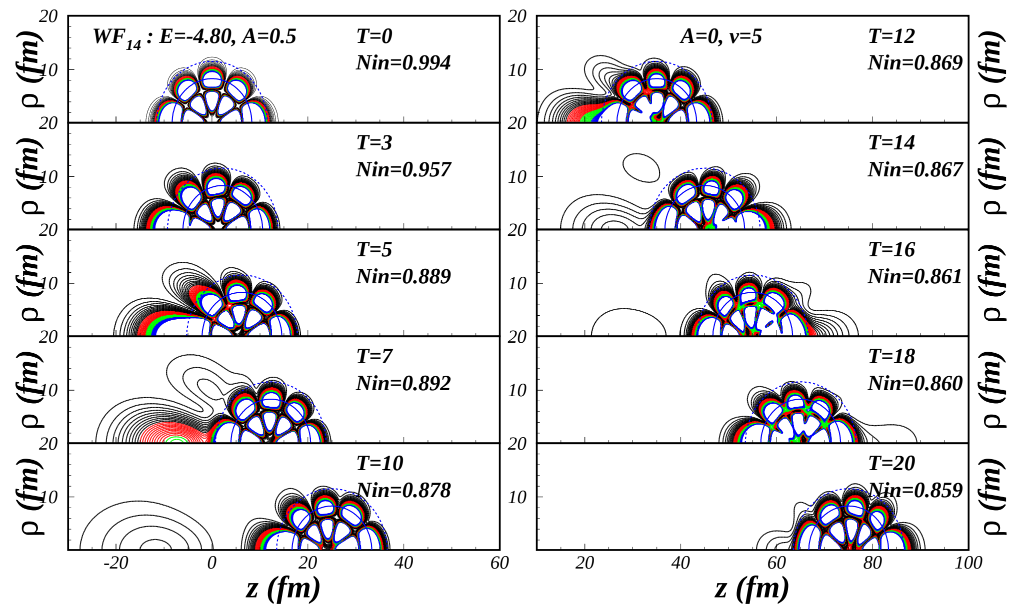


Figure 1: Time evolution of $|\Phi_{14}^0|^2$ during (left) and after (right) acceleration for spherical $^{236}U$. $N_{in}$ is the norm inside the dotted circle defined by $V_0/100$. T is the time in $10^{-22}$ sec.

has a quantum origin. It is known that the tunneling path of a metastable state is mainly dictated by its quantum numbers [14, 15]. In other words the emission preserves the spatial distribution of the respective state. Hence we expect a 2nd peak at 125° in the nuclear system which translates into an emission at 150° in the laboratory system.

Figs. 2 and 3 show the time dependence of two other neutron states with energies below (-8.3 MeV) and above (-3.4 MeV) the Fermi level respectively. The wave function with lower energy oscillates during both regimes: quadratic and linear $\alpha(t)$. It doesn't however succeed to escape: its presence inside the nucleus is practically unchanged. On the contrary, 49% of the wave function with higher energy is emitted, in the same interval of time, through strong oscillations. Predictably, the emission starts earlier and is more intense. As for $\Phi_{14}^0$, there are also two directions of emission: one intense at 180° and one weak at an angle between 180° and 90°.

For a better understanding of the physics involved, we divide the total energy in the laboratory system in significant terms:

$$\langle\Phi|H|\Phi\rangle = -\frac{h^2}{2m}\int\int\left(\Psi^*\frac{\partial^2\Psi}{\partial\rho^2}+\Psi^*\frac{\partial^2\Psi}{\partial q^2}\right)d\rho dq+\frac{h^2}{2m}b^2\dot{\alpha}^2\int\int|\Psi|^2 d\rho dq$$

$$-\frac{h^2}{2m}2ib\dot{\alpha}\int\int\Psi^*\frac{\partial\Psi}{\partial q}d\rho dq+\frac{h^2}{2m}\left(\Lambda^2-1/4\right)\int\int\frac{1}{\rho^2}|\Psi|^2 d\rho dq+\int\int V(\rho,q)|\Psi|^2 d\rho dq. \tag{8}$$

The 1st term is the average kinetic energy in the nuclear frame. The 2nd term reduces to $m\dot{\alpha}^2/2$; it is the extra kinetic energy due to the velocity of the potential. The 3rd

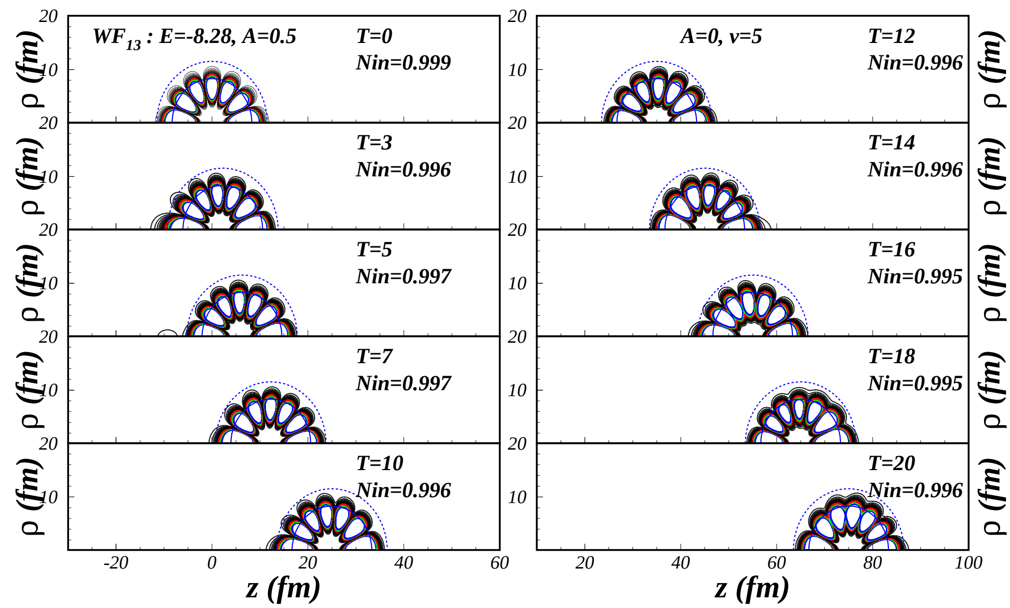


Figure 2: The same as in Fig. 1 but for $\Phi^0_{13}$.

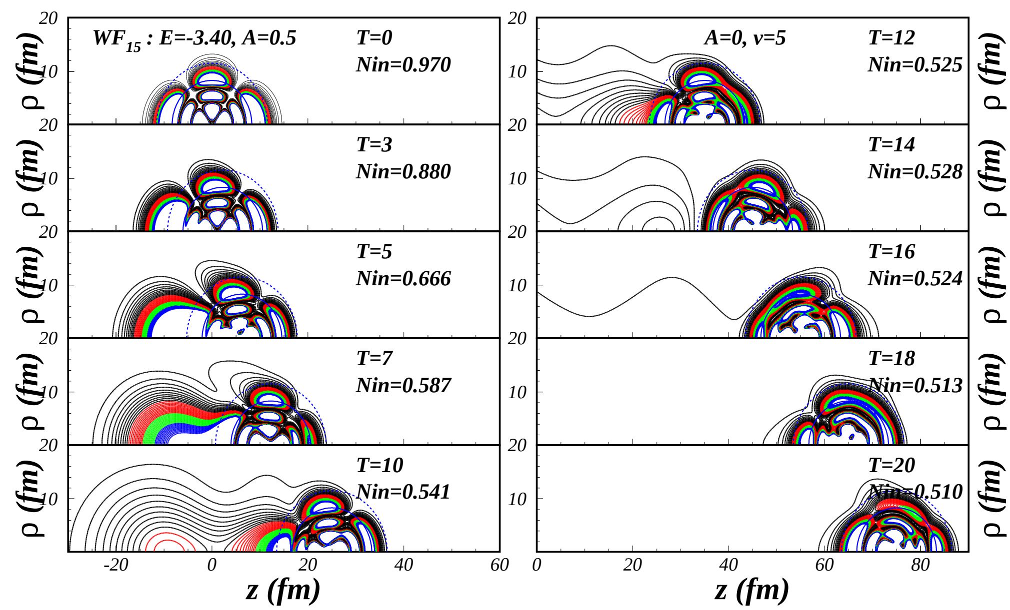


Figure 3: The same as in Fig. 1 but for $\Phi^0_{15}$.

term reduces to $\dot{\alpha} < p >$ where $< p >$ is the average momentum in the nuclear frame.

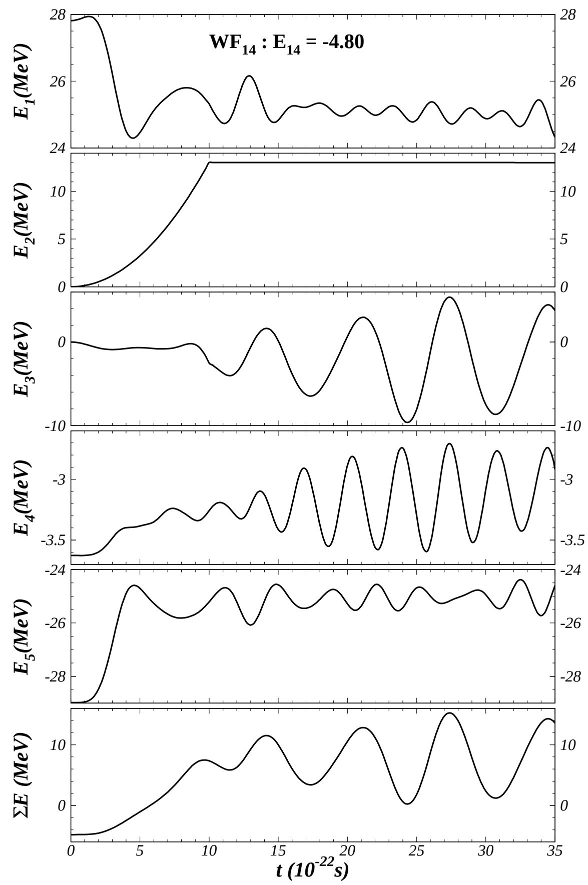


Figure 4: The five terms which form the neutron energy in the laboratory system.

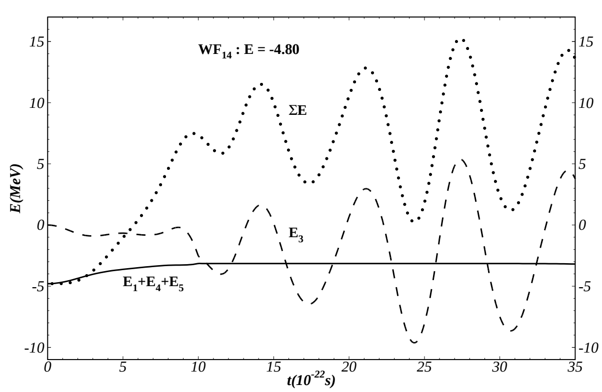


Figure 5: The neutron energy in the laboratory system (dotted line), in the nuclear system (solid) and the energy due to the interaction with the moving potential (dashed).

It represents the variation of the neutron energy due to the interaction with the moving wall of the potential; equivalent to the "one-body" dissipation [11]. The last two terms are the average centrifugal and nuclear potentials respectively.

These 5 terms as well as their sum are plotted in Fig.4 as a function of time for the neutron state close to the Fermi energy. Their variation during acceleration is explained by two facts: a) the emitted fraction of the wave packet is more and more present in the nuclear surface or even outside the nucleus. This e.g., diminishes E1 and boosts E4 and E5. b) the emission is accompanied by an oscillatory motion. From the variation of E2, one observes that our neutron reaches 13 MeV in $10^{-21}$ sec. In a linear accelerator a $^{236}$U ion can easily attain the same velocity but in a much longer time.

After T=10 there is only this oscillatory motion left. The sum E1+E4+E5 i.e., the neutron energy in the nuclear frame, is constant and the oscillations of E are due only to E3 as clearly seen in Fig.5.

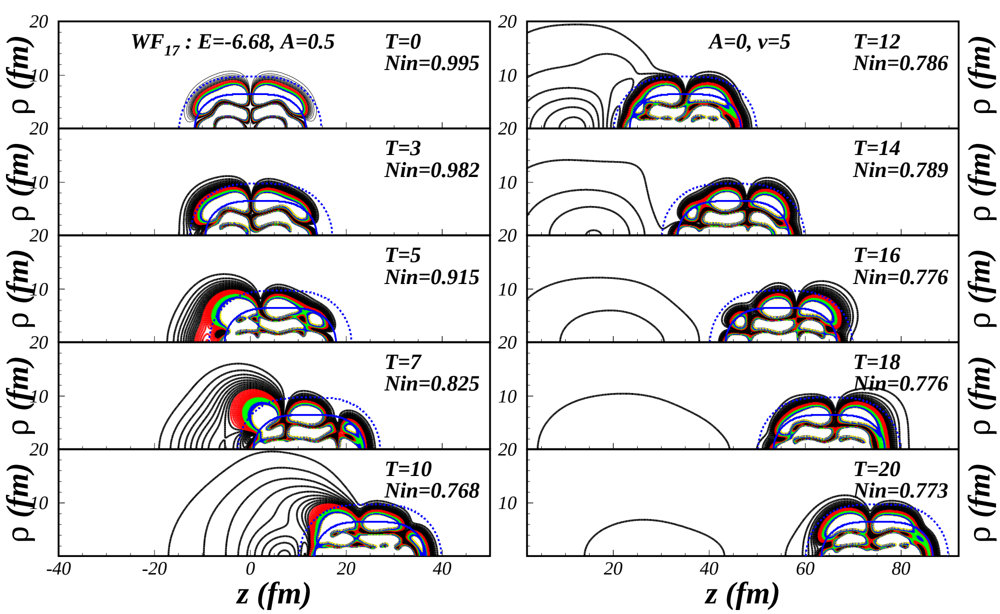


Figure 6: Time evolution of $|\Phi^0_{17}|^2$ during (left) and after (right) acceleration for the shape isomer (deformation parameter $\epsilon$=0.52) of $^{236}U$. $N_{in}$ is the norm inside the dotted ellipse defined by $V_0/100$. T is the time in $10^{-22}$ sec.

Finally we study the effect of nuclear deformation on the neutron emission due to acceleration of the nucleus along the deformation axis. For this we describe the nuclear shape by a pure Cassini oval with deformation parameter $\epsilon$=0.52. It is the shape isomer of $^{236}U$ [16]. The results for two neutron states, one below and one above the Fermi level, are presented in Figs. 6 and 7 respectively. The emission probability is again larger in the latter case: $N_{in}$ = 0.39 vs 0.77. One can also notice that the emission at angles smaller than 180° to the z-axis is much intenser than in the previous cases. It is because a quasi-stationary state in a deformed nucleus tunnels most probably pependicularly to

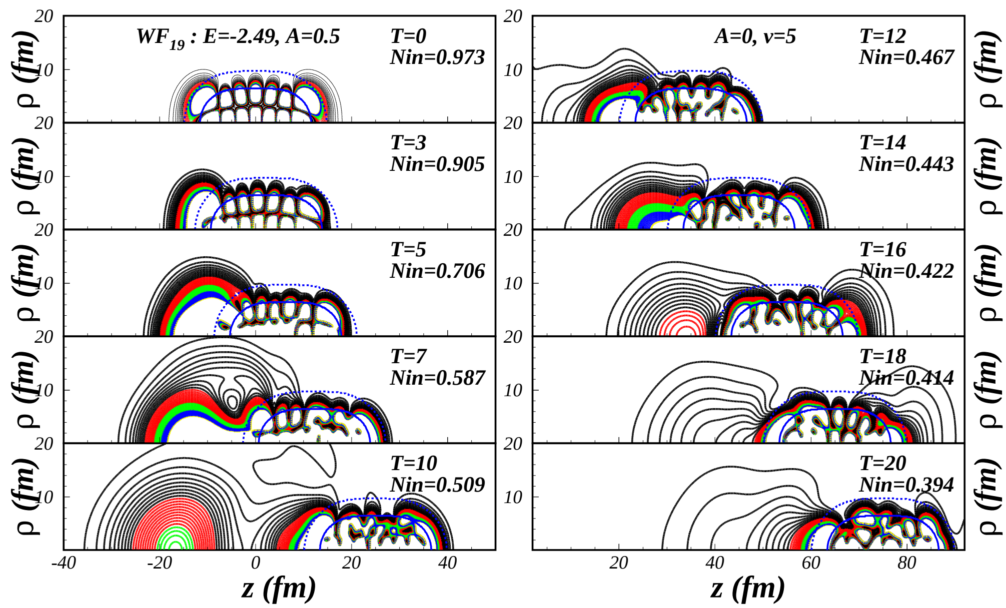


Figure 7: The same as in Fig.6 but for $|\Phi^0_{17}|^2$.

the deformation axis [17], irrespective if the barrier is lower or higher along this direction. It is what happens here: the emission occurs at 90° in the nuclear system. Due to the displacement of the nucleus however, in the laboratory system, the emission occurs at slightly larger angles ($\approx 110°$). Hence there is qualitative difference between spherical and strongly deformed nuclei: in the latter case, the direction imposed by quantum mechanics competes in intensity with the classically expected direction of emission.

## 5. Concluding remarks

A similar emission takes place during the slowing down (A<0) of a projectile when it approaches a target. Among possible effects, an increase of the neutron-transfer cross section is expected. The value chosen (A=0.5) is larger than the acceleration during the Coulomb repulsion of two equal fission fragments from $^{236}$U separated by $D_{cm}$= 20 fm (A=0.13) but comparable with that attained during the collision of two $^{236}$U nuclei at the same distance of approach (A=0.52). In conclusion, there is probably no acceleration induced excitation of the fission fragments during their separation. On the other hand, a heavy projectile is expected to become excited (even to emit neutrons) when it approaches a heavy target or moves away from it. However, the acceleration produced in Coulomb interactions is not constant (it depends on $D_{cm}$) and a high level cannot be maintained for $10^{-21}$ sec, a long time at the scale of the above mentioned processes. For a quantitative answer a dedicated study is necessary.

The process of acceleration induced neutron emission has similarities with the realease of neutrons at scission i.e., during the last stage of nuclear fission. They are both due to a fast change of the potential in which they move that transforms each neutron state into a wave packet with components in the continuum [12, 13]. In the case of scission neutrons however, it is the shape of the potential and not its position that changes.

**Acknowledgements**

We are grateful to Gurgen Ter-Akopian and Jorgen Randrup for their interest in this work and illuminating discussions. This work was done in the frame of the projects PN-III-P4-ID-PCE-2016-0649 (contract nr. 194/2017) and PCE-2016-0014 (contract nr.7/2017).

# References

[1] M. Goeppert-Mayer, J.H.D. Jensen, *Nuclear Shell Structure* (John Wiley and Sons, New York, 1955).

[2] H. Wiedemann, *Particle Accelerator Physics* (Springer, Berlin, 1999).

[3] P. Rouchon, *Control of a quantum particle in a moving potential well* in: *Proceedings of the 2nd IFAC Workshop on Lagrangian and Hamilton Methods for Nonlinear Control, Seville, 2003* p.317.

[4] K. Beauchard, J.-M. Coron, *Controllability of a quantum particle in a moving potential well*, J. Functional Analysis **232**, 328 (2006).

[5] S. Miyashita, *Conveyance of a quantum particle by a moving potential well*, J. Phys. Soc. Japan **76**, 104003 (2007).

[6] A.G. Butkovsky, Y.I. Samoilenko, *Control of Quantum- Mechanical Processes and Systems*, Vol.56 of *Mathematics and its Applications (Soviet Series)*, (Kluver Academic Publishers Dortrecht/Boston/London. English edition, 1990).

[7] C-C Chou, R.E. Wyatt, *Time-dependent Schrodinger equation with Markovian outgoing wave boundary conditions: Applications to quantum tunneling dynamics and photoionization*, Int. J. Quantum Chem. **1**13, 39 (2013).

[8] C. R. Jesshope, *SIPSOL - suite of subprograms for the solution of the linear equations arising from elliptic partial differential equations*, Comp. Phys. Commun. **17**, 383 (1979).

[9] E. Rost, *Proton shell-model potential for lead and the stability of superheavy nuclei*, Phys. Lett. B **26**, 184 (1968).

[10] S. A. Gurwitz, G. Kalberman, *Decay width and shift of a quasistationary state*, Phys. Rev. Lett. **59**, 262 (1987).

[11] J. Blocki, Y. Boneh, J. R. Nix, M. Robel, A.J. Sierk, W. J. Swiatecki, *One-Body Dissipation and the Super-Viscidity of Nuclei*, Ann. of Phys. **113**, 330 (1978).

[12] M. Rizea, N. Carjan, *Dynamical Scission Model*, Nuc. Phys. A **909**, 50 (2013).

[13] N. Carjan, M. Rizea, *Similarities between calculated scission-neutron properties and experimental data on prompt fission neutrons* , Phys. Lett. B **747**, 178 (2015).

[14] P. Talou, N. Carjan, D. Strottman, *Time-dependent approach to bidimensional quantum tunneling: application to the proton emission from deformed nuclei*, Nuc. Phys. A **647**, 21 (1999).

[15] N. Carjan, P. Talou, D. Strottman, *Angular distribution of protons emitted from oriented nuclei: toward imaging single-particle wave functions*, *The Nucleus: New Physics for the New Millenium*, Eds. Smit et al., (Kluver Academic/Plenum Publishers, New York, 2000) p 115.

[16] V. Pashkevich, *On the asymmetric deformation of fissioning nuclei*, Nucl. Phys. A **169**, 275 (1971).

[17] D. Strottman, N. Carjan, P. Talou, *New Aspects in the Decay of Quasi-Stationary States by Multidimensional Tunneling*, Physica Scripta **T88**, 148 (2000).